Diffusion with evolving sources and competing sinks: Development of angiogenesis

M. Scalerandi and B. Capogrosso Sansone
INFM, Dipartimento di Fisica, Politecnico di Torino, Torino, Italy

C. A. Condat
FaMAF, Universidad Nacional de Córdoba, 5000-Córdoba, Argentina
and Department of Physics, University of Puerto Rico, Mayagüez 00681, Puerto Rico
(Received 27 July 2001; published 14 December 2001)

Tumors ensure their long-time growth by emitting molecular messengers that induce cellular modifications in neighboring capillaries. These modifications are conducive to the enlargement of the vascular system feeding the tumor. This phenomenon, termed angiogenesis, is controlled by the diffusion and competitive trapping of nutrients and molecular messengers by several cell species. The number, location, and properties of these traps change continuously. The angiogenic process also implies that nutrient sources are time dependent. Starting from assumptions at the cellular level, we formulate a mathematical model that predicts the evolution of angiogenesis and the increase in the blood flow to the tumor. The model also predicts the emergence of directed growth and the possibility of therapeutical synergy. Simulations permit a careful analysis of the influence of the main parameters.

DOI: 10.1103/PhysRevE.65.011902 PACS number(s): 87.10.+e, 02.60.Cb

I. INTRODUCTION

A frustrating element in the fight against cancer is acquired drug resistance, which is found in 30% of all patients undergoing chemotherapy [1]. Acquired drug resistance is generated by the ability of cancer cells to adapt and modify. In 1997, a paper by Boehm, Folkman, Browder, and O'Reilly [2] showed that a very promising avenue to treat cancer would be to inhibit angiogenesis, i.e., the growth of the vascular system feeding the tumor. This possibility arises because endothelial cells, the progenitors of the new capillaries, are genetically more stable than tumor cells, and thus much less capable of acquiring drug resistance [1]. Vascular growth is not only generally necessary for the growth of primary tumors, but it is also a condition for the successful implantation of metastases [3]. Indeed, microvessel density is a significant prognostic indicator [4]. Therefore, it is not surprising that there is now intense experimental activity directed at characterizing and optimizing antiangiogenic therapies and procedures [5–13]. Crucially, animal experimental models suggest that the synergistic interaction of different inhibitors may pave the way for effective anticancer therapies [5,7,10]. In this context, we note that different angiogenesis inhibitors have been found to have different efficacies depending on the angiogenesis stage being targeted [10]. It would be therefore profitable to have a manageable mathematical model that permitted the visualization of angiogenesis and the evaluation of the influence of variations in the relevant parameters. We have recently developed such a model, indicating how therapeutical synergy may develop and how directional growth may emerge [14]. In this paper we perform a careful analysis of the model, investigating the importance and meaning of various parameters, particularly for what concerns the reasons for the eventual failure of angiogenesis, and presenting a more detailed physical picture. We also include and discuss the full set of discrete iteration equations that we use to implement the model.

In the early stages of cancer growth, tumor cells take their oxygen and nutrients directly from their immediate environment. These cells multiply and the tumor grows. When it reaches a size of a few milimeters, or even before, cancer cells, which compete for the available nutrients, begin to starve. They release one or more molecular messengers [4,15], which we will generally refer to as ''tumor angiogenic factors'' (TAFs). Two very studied angiogenic messengers are fibroblast growth factor (FGF) and vascular endothelial growth factor (VEGF)—the interaction between VEGF and its receptor on the cell surface being central to the evolution of the embryonic vascular system [11,12]. These messengers signal the endothelial cells lining the capillaries in the tumor vicinity that they must reproduce and move. Following their instructions, these cells combine to form sprouts, which grow and rearrange to extend the tumor-feeding structure [16]. The remodeling and consolidation of this structure is accompanied by the enlargement and division of preexisting vessels, which ensure the ability of the capillary net to feed the tumor. After rearrangement and pruning, the emerging vascular net resembles a mature vessel system [16]. The tumor, now well fed, resumes growth at a fast rate.

Several models have been recently developed for the nonvascular stage of cancer growth [17–24]. In our own model we stressed the importance of the competition for nutrients in determining tumor morphology and growth rate [21]. Here we will show that competition for nutrients is also a determinant for vascular growth. As a rule, there will be a delay between the start of the TAF diffusion into healthy tissue and the increase in the amount of nutrient reaching the tumor. This delay is due to various cellular processes needed for the expansion and consolidation of the capillary net. Endothelial cells (ECs) evolve to fulfill different roles during angiogenesis. According to their function, we can consider three types of ECs: detached ECs that migrate towards the TAF source, coalescing ECs that form unstable sprouts, and ECs that be-

long to stable, blood-transporting vessels. We will consider these three populations separately, introducing explicit rules for the transformations between species. Different cell species will compete for nutrients and for the TAF.

In 1991, Stokes, Lauffenburger, and Williams formulated an angiogenesis model in which sprouts grew following the path of a single migrating cell [25]. They showed that, in a purely dynamic model, chemotaxis is needed to orient vascular growth towards the tumor. In this paper we will show that new vessels grow in the direction of the tumor even in the absence of chemotaxis, if we take into account the effects of the TAF on nutrient utilization: the TAF modifies some cellular processes, redirecting the use of energy and favoring reproduction (i.e., acting as a growth factor). Therefore, reproduction rates will tend to be higher in regions containing higher TAF concentrations. As a consequence, the TAF behaves as a mitogenic factor and then, even if no bias is explicitly introduced for cell transport, the capillary net grows towards the tumor.

In their recent work, Holmes and Sleeman analyzed in detail the influence of mechanical factors, notably cellular traction and viscoelasticity, on the development of angiogenesis [26]. In this paper we adopt a different point of view, examining how the competition between the various cell species for the TAF and nutrients impacts the development of the extended vascular net, whereas pressure is explicitly taken into account only as an inhibitor of cell reproduction. We will not be interested in predicting a detailed vascular configuration, which would not be very useful in any case, but on providing averaged predictions for the spatiotemporal dependence of cell concentrations and for the angiogenesis-induced increase in the amount of nutrient available to the tumor.

Since different angiogenic inhibitors are likely to act upon different stages of the angiogenic process [10], it is reasonable to think that their action modifies different model parameters. We have explored how the variation of some of the most relevant parameters influences the evolution of the vascular system feeding the tumor. To optimize this process would mean to increase the transport of nutrients to the tumor as much as possible with as little an expenditure as possible on the expanded vascular system. We will characterize the success of the process by defining an angiogenic efficiency.

In principle, the physical problem is daunting: We have two diffusing species, the nutrients and the TAF. Both can be trapped by various cell types: nutrients by all cells and the TAF by the three EC species. Migrating ECs are really moving sinks that carry the absorbed nutrient along [27]. Cellular division and death imply the nonconservation of the sink number and the partition of the energetic resources, whereas cell transformations imply that nutrients (and energy) flow from one cell species to another. Additionally, sources are time dependent, because the number and distribution of blood-transporting vessels changes with time. Although the theory of trapping kinetics under various conditions has advanced a great deal in the last few years [28], the problem presented here is certainly unmanageable by analytic techniques. Fortunately, the model equations can be constructed in a form suitable for their computational solution using the local interaction simulation approach (LISA) [29,30]. In this approach, the model is directly implemented in terms of discrete iteration equations, which allows for its easy adaptation to different situations and geometric constraints.

II. THE MODEL

Blood vessels that initially run in the tumor vicinity will be assumed to be the initial sources of mobile endothelial cells. After the extended vascular net has grown in such a way that the tumoral cells become again sufficiently irrigated, they interrupt TAF production and the vascular net evolves towards its final configuration. Of course, once the tumor increases its volume substantially, new vascular growth is likely to be required, and there will be a continuous feedback between growing tumor and augmented vascular system. Our angiogenesis model will describe the initial stages of vascular growth. It is built upon the following assumptions [14].

(a) Starving tumor cells generate the TAF.

(b) The TAF diffuses in the region surrounding the tumor and signals the ECs to move and reproduce. New ECs (c_1) can also migrate and reproduce. Chemotaxis is not explicitly introduced.

(c) Mobile ECs (c_1) can coalesce in tubes and sprouts forming temporary structures. We consider tube-forming cells as members of a new species (c_2).

(d) Once the local EC concentration is sufficiently high, the structures stabilize and become blood transporting. Cells belonging to permanent structures will be labeled c_3. Vessel connectivity must be ensured, i.e., the transformation $c_2 \rightarrow c_3$ is allowed only when there are preexisting c_3 cells in the immediate neighborhood.

(e) Energy utilization is redirected in ECs detached from vessels, facilitating reproduction. ECs may reproduce if they contain enough stored energy. Daughter cells always belong to the c_1 species.

(f) TAF generation is inhibited once the total nutrient reaching the tumor surpasses a certain threshold.

(g) Healthy nonendothelial cells (HNECs) play a passive role and are represented by a constant, uniform nutrient sink.

To implement the model, we consider a piece of tissue, which we discretize into identical elements. Each element is represented by a node $\vec{i}$ located at its center. Cells belonging to four different populations may occupy element $\vec{i}$ at time t; in addition to a fixed number $c_0(\vec{i})$ of HNECs, we may have three endothelial cell types: Detached (or free) cells that may migrate through the tissue $[c_1^t(\vec{i})]$, cells belonging to tubes without blood flow $[c_2^t(\vec{i})]$, and cells belonging to blood-conducting vessels $[c_3^t(\vec{i})]$. We also associate with each node the concentrations $v^t(\vec{i})$ of the TAF and $p^t(\vec{i})$ of free nutrients.

In the following sections we specify the rules that determine the spatiotemporal evolution of cells and capillaries. Several processes take place: for the molecular species, diffusion, absorption, and consumption of nutrients and the

TAF; for the cell species, mitosis and cell transformations. Since diffusion is very fast compared to the other processes, we will implement it at every time step in the simulation, while absorption, consumption, mitosis, and cell transformations, which are linked to the slower cell metabolism will be implemented only every T time steps. The variable $\vec{i}$ will be omitted in what follows whenever no ambiguity ensues.

A. Diffusion

Iteration equations describe the change in molecular concentrations from time t to time $t+\tau$ due to diffusion. For the nutrients we write

$$p^{t+\tau}(\vec{i}) = p^t + \alpha_p \sum_{\vec{n}} [p^t(\vec{n}) - p^t] + S_p^t - \Xi_p, \qquad (1)$$

where $\vec{n}$ denotes one of the nearest neighbors and α_p is the nutrient diffusion coefficient. For simplicity, a single nutrient species is considered; to introduce more species would be elementary, although cumbersome. S_p^t is the source term, which is nonzero only at those locations where blood-transporting vessels are present. It is proportional to the permeability of the vessel wall and to the local vessel surface area (and hence to c_3). Ξ_p is a sink for the nutrient that represents its uptake by HNECs.

TAF diffusion is described by

$$v^{t+\tau}(\vec{i}) = (1-\xi_v)v^t + \alpha_v \sum_{\vec{n}} [v^t(\vec{n}) - v^t] + S_v^t, \qquad (2)$$

where α_v is the TAF diffusion coefficient, S_v^t is the TAF source term, which is nonzero only at the tumor location, and ξ_v characterizes the decay of unbound TAF. The TAF source will be active until the nutrient suffices to provide for the cancer cell needs. The simplest choice is to assume that S_v^t is a constant while the source is active. Of course, other choices would be possible. For instance, TAF production could depend on the difference between the instantaneous nutrient concentration at the tumor location and the concentration that tumor cells find to be ideal for their development. Alternatively, the TAF source could be on for a fixed time (simulating, e.g., *in vitro* experiments). Nutrient and TAF absorption by endothelial cells is introduced below.

The migration of free endothelial cells, c_1, is characterized by a diffusion coefficient α_1,

$$c_1^{t+\tau}(\vec{i}) = c_1^t + \alpha_1 \sum_{\vec{n}} [c_1^t(\vec{n}) - c_1^t]. \qquad (3)$$

Other cell species are not allowed to move.

B. Absorption and consumption

As relatively slow processes, absorption and consumption are calculated only every T time steps. In practice we divide the time interval $[t, t+\tau]$ into the two subintervals $[t, t']$ and $[t', t+\tau]$, where $t = nT$ (n is an integer) and $t' = t + \tau/2$. Absorption is simulated during the first interval $[t, t']$, while the second interval is reserved for cell proliferation and transformation.

Nutrient absorption is carried out by cell receptors; the absorbed nutrient is transformed into stored energy σ_k^t. The number of receptors formed by each cell is defined by the required amount of nutrients: cells consuming more nutrients develop a larger number of receptors. Let Γ_k be the maximum nutrient uptake by a single cell in species k during each time step $t \to t'$, expressed in energy units. In general, the number of receptors on the cell surface is larger than the minimum required to perform the task assigned to the cell. However, not every receptor is active, since activation depends on the nutrient concentration in the cell neighborhood. The energy absorbed by a single cell belonging to the kth population ($k = 1,2$) is

$$\gamma_k^t = \Gamma_k \left\{ 1 - \exp\left[- \frac{p^t}{\sum_{l=1}^{2} \Gamma_l c_l^t} \right] \right\}. \qquad (4)$$

The factor inside the curly brackets was introduced to keep track of the partial inactivation of the receptors. It is proportional to p^t for low nutrient concentrations, while it tends to unity for high nutrient concentrations. Since cells belonging to capillary walls (c_3) take their nutrient directly from the blood flow, they do not compete with other cells. Instead they sense always an inexhaustible amount of nutrient. As a consequence, each cell in this population absorbs an amount of nutrient $\gamma_3^t = \Gamma_3$. The total nutrient absorbed by all cells of species k in element $\vec{i}$ is $\gamma_k^t c_k^t$. The concentration of free nutrient is correspondingly decreased,

$$p^{t'} = p^t - \sum_{k=1}^{2} \gamma_k^t c_k^t. \qquad (5)$$

In normal conditions (no external signals) we may assume that the cells are in a steady state and we can simply write $\gamma_k^t = \beta_k^t$, with β_k^t being the total energy *consumed* by each cell to perform its metabolic functions during the time step. When the external signal (TAF) is introduced, the cell metabolic functions are modified; in particular, energy resources must be allotted for reproduction. As a consequence, it is convenient to divide the rate of nutrient consumption into two parts,

$$\beta_k^t = \beta_{0,k} + \beta_{1,k} \exp[-\chi_k G_k^t] \qquad (6)$$

($k = 1,2,3$), where $\beta_{0,k}$ is the portion of metabolic consumption that is not affected by the signal (basal metabolic rate). The second term on the right-hand side is the portion that depends on the rate of TAF absorption. The parameters β_{1k} and χ_k characterize the strength of TAF influence on cell metabolism, whereas G_k^t represents the rate of TAF absorption by each cell belonging to the kth species. This rate is linearly dependent on the local TAF concentration v^t and on an absorption coefficient ζ_k, which is proportional to the number of active TAF receptors in each cell,

$$G_k^t = \zeta_k v^t \Big/ \sum_{l=1}^{3} c_l^t . \tag{7}$$

Due to its absorption by the various EC species, the concentration of extracellular TAF is reduced according to

$$v^{t'} = v^t - \sum_{k=1}^{3} c_k^t G_k^t . \tag{8}$$

The amount $\sigma_k^{t'}$ of stored energy per cell is determined by the balance between the amounts of energy absorbed per cell (γ_k^t) and consumed to perform cellular metabolic functions (β_k^t),

$$\sigma_k^{t'} = \sigma_k^t + \gamma_k^t - \beta_k^t .$$

C. Cell proliferation and death

The dynamics of nutrient absorption and consumption in the presence of the TAF has a strong influence on cell populations. While the absence of stored nutrient will cause cellular death, an increase of the stored nutrient beyond the mitosis threshold M_k will allow cells in species k to multiply. As a consequence, cell evolution will depend on the amount of stored nutrient at time t', $\sigma_k^{t'}$. Defining the energy scale so that the apoptosis threshold corresponds to $\sigma_k^{t'}=0$, three situations can occur.

(1) If $\sigma_k^{t'}<0$, cellular death (apoptosis) takes place. The number of eliminated cells increases with the nutrient defect. We write

$$c_k^{t'} = \frac{\sigma_k^t + \gamma_k^t}{\beta_k^t} c_k^t - \xi_k c_k^t . \tag{9}$$

Since c_1 and c_2 cells have limited life cycles, we introduced the intrinsic death rates ξ_1 and ξ_2. On the other hand, HNECs and c_3 cells have long lifetimes and we can assume that $\xi_0=\xi_3=0$. The coefficient of the first term in the right-hand side of Eq. (9) ensures that the surviving cells are left with (just) the amount of stored energy required to perform their metabolic function, i.e., after the occurrence of apoptosis the cells surviving in the element have $\sigma_k^{t'}=0$.

(2) If $0 \leqslant \sigma_k^{t'} \leqslant M_k$, cells will neither starve nor multiply, their number being merely reduced by aging. Therefore, the cell concentrations evolve according to

$$c_k^{t'} = c_k^t - \xi_k c_k^t . \tag{10}$$

(3) If $\sigma_k^{t'} > M_k$, cellular proliferation occurs, yielding additional c_1 cells. The concentration for these evolves according to the rule

$$c_1^{t'} = [1-\xi_1] c_1^t + \sum_{k=1}^{3} \lambda_{d,k} \left\{ 1 - \tanh\left[\Psi \sum_l c_l^t \right] \right\} c_k^t , \tag{11}$$

where $\lambda_{d,k}$ is the duplication rate of the kth species. The tanh term was introduced to account for pressure effects (effective proliferation will be hindered by an increase in the number of preexisting cells). The importance of these effects is measured by the parameter Ψ. The evolution rules for the other two species are simply

$$c_2^{t'} = [1-\xi_2] c_2^t \tag{12}$$

and

$$c_3^{t'} = c_3^t . \tag{13}$$

Proliferation implies a redistribution of the energy stores. The amount of stored energy is also reduced because of mitosis-related consumption. We call the amount consumed per duplication W_k. The nutrient redistribution equations are easy to obtain but cumbersome. We only write down the equation corresponding to the redistribution when the parent cell belongs to the c_1 class,

$$\sigma_1^{t'} = \sigma_1^t \left[1 - W_1 \frac{c_1^{t'} - c_1^t}{c_1^t} \right] \frac{c_1^t}{c_1^{t'}} . \tag{14}$$

D. Cell transformations

Under suitable conditions, ECs evolve through different types. In the simulations these transformations are assumed to occur once every T time steps, following proliferation, in the intervals ranging from $t'=nT+\tau/2$ to $t+\tau=nT+\tau$. In each of these intervals, we introduce an intermediate time t_1 and perform two sequential steps.

(1) Transformation from free cells to tube-forming cells ($t' \to t_1$). It occurs when the local concentration of free cells is higher than a given threshold ($c_1^{t'} > Q_{ft}$). This transformation, which takes place at a rate λ_{ft}, is described by the following set of equations:

$$c_1^{t_1} = [1 - \lambda_{ft} \Theta(c_1^{t'} - Q_{ft})] c_1^{t'} ,$$

$$c_2^{t_1} = c_2^{t'} + \lambda_{ft} \Theta(c_1^{t'} - Q_{ft}) c_1^{t'} ,$$

$$\sigma_2^{t_1} = [c_2^{t_1}]^{-1} [\sigma_2^{t'} c_2^{t'} + \lambda_{ft} \Theta(c_1^{t'} - Q_{ft}) \sigma_1^{t'} c_1^{t'}] ,$$

$$\sigma_1^{t_1} = \sigma_1^{t'} .$$

Note that the energy stored in the transforming c_1 cells is redistributed among tube-forming cells. No sizable amount of nutrient is assumed to be consumed in the transformation process itself. Since *in vitro* experiments show that isolated ECs may form tubes [4], i.e., tube formation is not necessarily a collective effect, we take $Q_{ft}=0$.

(2) Transformation from tube-forming cells to vessel wall cells ($t_1 \to t+\tau$). It occurs when the local concentration of tube-forming cells is sufficiently high. The corresponding

threshold Q is then defined by adding the number of vessel-forming cells already present. The number ω of transformed cells is then

$$\omega = \Lambda c_2^{t_1} \Theta[c_2^{t_1} + c_3^{t_1} - Q], \tag{15}$$

where Λ is the transformation rate and Θ is Heaviside's step function. Of course, vessel connectivity must be ensured, so we must also require that $c_3^{t_1} \neq 0$ at least at one of the neighboring nodes. The new interconnected structures increase the local nutrient transport capacity of the vascular system. This induces the effective widening of the blood vessels feeding the augmented net, and an increase in the blood flow into the adjoining tumor. The proposed mechanism mimics the increase of the net lateral surface (which is locally proportional to c_3) as we move away from the original vessels. This increase is consistent with the observation that far from the original vessels there is a large number of thinner capillaries. The equations for the cell populations are

$$c_3^{t+\tau} = c_3^{t_1} + \omega,$$

$$c_2^{t+\tau} = c_2^{t_1} - \omega.$$

We have again a redistribution of stored nutrient,

$$\sigma_3^{t+\tau} = [c_3^{t+\tau}]^{-1} [\sigma_3^{t_1} c_3^{t_1} + \omega \sigma_2^{t_1}],$$

$$\sigma_2^{t+\tau} = \sigma_2^{t_1}.$$

E. Efficiency

Arguably, nature will try to optimize the benefits of the angiogenic process (from the point of view of the tumor) while at the same time minimizing its costs. The benefit is clearly the increase in the amount of nutrient available to the tumor. We will estimate this increase by looking at the variation in the quantity of free nutrients in the region of direct contact with the tumor. A measure of the cost is the increase in the total number of endothelial cells that is required to support the delivery of this additional nutrient. We can thus define the (unnormalized) efficiency e of the angiogenic process as [14]

$$e = \left(\frac{1}{C}\right) \frac{\sum_{\vec{m}} [p_{\vec{m}}(t \to \infty) - p_{\vec{m}}(t=0)]}{\sum_i p_{\vec{m}}(t=0)}, \tag{16}$$

where $\Sigma_{\vec{m}}$ runs over all the cells located at the tumor edge. The dimensionless cost C is defined as

$$C = \frac{\sum_{i,j} [c_{i,j}(3, t \to \infty) - c_{i,j}(3, t=0)]}{\sum_{i,j} c_{i,j}(3, t=0)}, \tag{17}$$

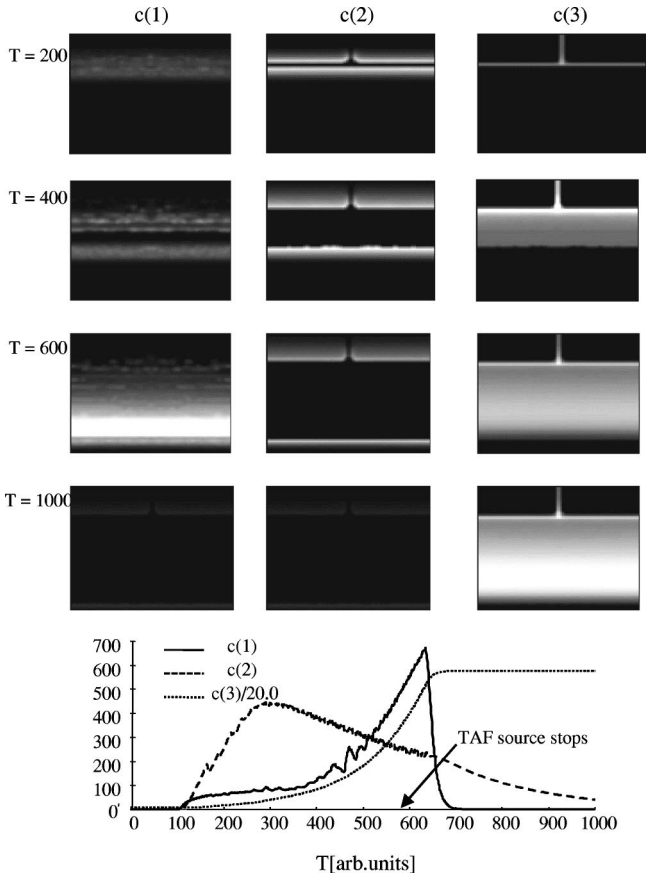

FIG. 1. Snapshots of the three endothelial species, c_1 (diffusing ECs), c_2 (tube-forming ECs), and c_3 (vessel ECs), taken at the indicated times. The initial vessel configuration is evident in the c_3 snapshots. The TAF-generating tumor abuts the lower edge of the figures. The linear plots represent the time evolution of the total cell number. The arrow indicates the time at which TAF generation is discontinued. See text for the parameter values.

where the sum now runs over the entire specimen. Of course, other definitions of efficiency are possible, but the one we present here is informative and simple to evaluate. We remark that the concept of efficiency has been recently used to characterize biophysical processes, such as the operation of molecular motors, under various conditions [31–33].

III. RESULTS AND DISCUSSION

Due to the complexity of the problem and the simultaneous presence of several cell species, the model necessarily contains several parameters. The value of these parameters will depend on the type and location of the tumor and on the nature and state of its environment. Some of the parameters will consequently change substantially from one specific tumor to another. We have examined the effects of the variations of those parameters, which are qualitatively most relevant. In all cases we took $T = 100\tau$. For simplicity, and in the absence of contradicting data, we have given some of the cellular parameters the same values for the three EC species considered. We have taken $\beta_{0k} = \beta_0 = 0.01$, $\lambda_{d,k} = \lambda_d = 0.5$,

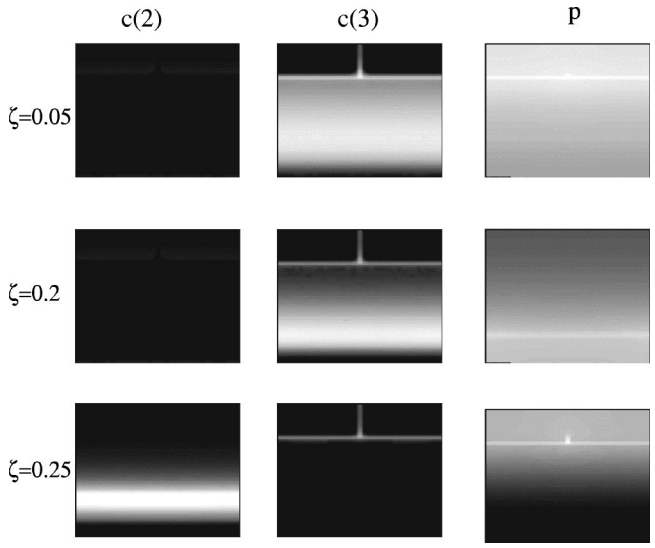

FIG. 2. Effects of changing the rate of TAF absorption (ζ). Snapshot rows correspond to the steady-state distributions for three different values of the TAF absorption coefficient. The rest of the parameters are as in Fig. 1. The columns represent, respectively, concentrations of unstable tube cells, stable structure cells, and free nutrients.

$M_k=M=0.5$, $\chi_k=\chi=40$, $W_k=W=0.05$, and $\zeta_k=\zeta$ for all k. Additionally, $\alpha_p=0.2$, $\alpha_v=0.1$, $\alpha_1=0.2$, $\lambda_{ft}=0.1$, $Q_{ft}=0$, $\Lambda=0.9$, $\Psi=1$, $\Gamma_3=0.1$, $\beta_{13}=0.09$, $\xi_1=\xi_2=0.005$, $\xi_v=0$, $\beta_{11}=\beta_{12}=0.03$, $\Gamma_1=\Gamma_2=0.04$, $\Xi_p=0.004$, $S_p=2$ wherever $c_3\neq 0$, and $S_v=0.2$ while the TAF source is active. The numerical values of the other parameters will be specified later, as needed. In all cases, TAF generation is stopped if the total amount of nutrient reaching the tumor edge is three times the original value. Typically, process completion requires between 10^5 and 2×10^5 diffusional steps.

Boundary conditions. The LISA method allows for an arbitrary choice of boundary and initial conditions, which could be adapted to any specific problem. For the figures presented here, we take a square $N\times N$ specimen, setting periodic boundary conditions at its left and right edges. The lower and upper edges, if tumor-free, will be TAF sinks and nutrient reflectors. Tumor edges will be nutrient sinks and TAF sources. c_1 cells are not allowed to penetrate the tumor.

Initial conditions. HNECs are uniformly distributed through the tissue. Thus, $c_0^t(\vec{i})=c_0$. The initial distribution of nutrients is obtained by letting the system evolve with the original capillaries but without any TAF source for a very long time, until steady-state conditions are reached. Tumor cells and nutrient sources may be arbitrarily distributed.

In order to perform a detailed study of the influence of the various parameters, we select a simple geometry. The initial capillaries form an inverted T, whose location is described by

$$c_3^0(i,j)=c_3^0[\,\delta_{j,3N/4}+(\,\delta_{i,N/2}+\delta_{i,N/2+1})\Theta(j-3N/4)], \tag{18}$$

where c_3^0 is the number of ECs forming the walls of the initial vessels and $\delta_{i,j}$ is the Kronecker delta. The tumor is assumed to be outside the specimen, abutting its lower edge.

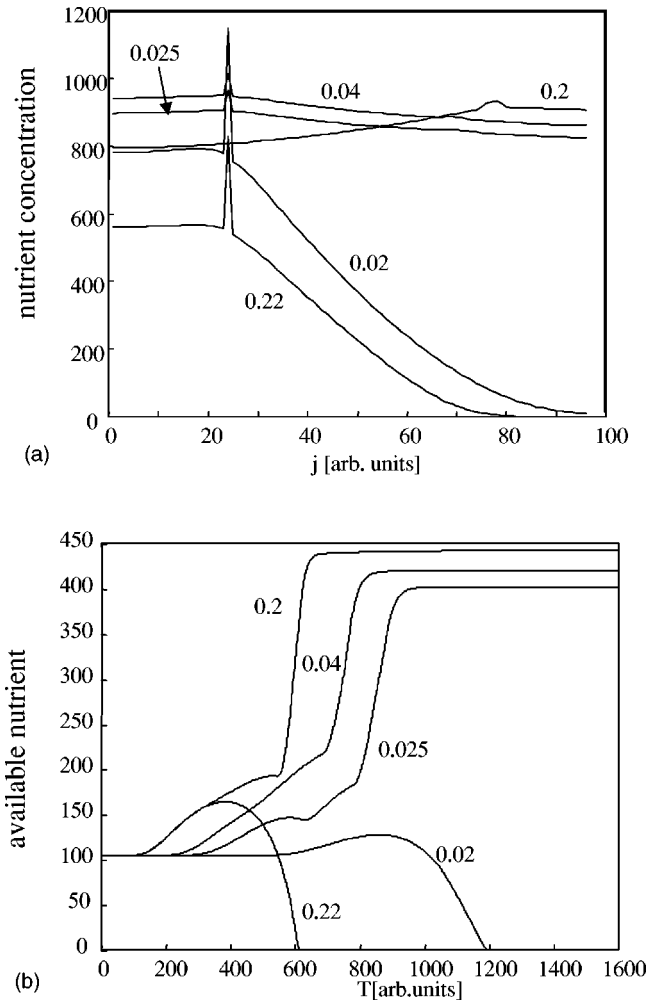

FIG. 3. (a) Available nutrient concentration profiles as functions of distance from the tumor. The original vessel is located at $j=25$ and the tumor surface is at $j=100$. (b) Total nutrient available to tumor as a function of time. The parameters are those in Fig. 1, except that ζ takes the values specified next to the corresponding curves.

Figure 1 shows snapshots of the endothelial cell concentrations for $Q=0.3$ and $\zeta=0.1$. The concentration of free, diffusing ECs (c_1) exhibits a front moving towards the tumor. Proliferation is fastest for sprout-leading cells, since TAF reaches them without being screened. Some of the c_1 cells transform into tube-forming (c_2) structures. Note that both cell species have almost disappeared by $T=1000$, when the final structure has consolidated. The evolution of the vessel-forming ECs (c_3) with a steady-state maximum in the tumor neighborhood is evidence of a successful angiogenic process. The time evolution of the total cell population in each species is described by the linear plots. Rapid cell reproduction in the nutrient-rich neighborhood of the original vessels gives rise to the fast increase in the c_1 and c_2 populations. The c_1 population peaks soon after TAF generation is stopped. The nonzero initial value of c_3 is due to the presence of the initial vessels.

The spatial distribution of free nutrients (not shown) can

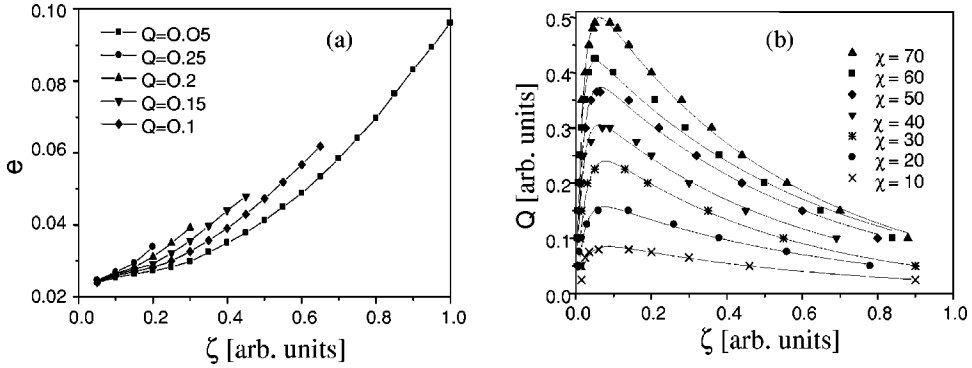

FIG. 4. (a) Angiogenic efficiency as a function of TAF absorption rate (ζ) for $\chi=40$ and the values of the transformation threshold Q detailed in the figure. (b) Regions of successful and failed angiogenesis in the parameter plane (ζ,Q) for the values of the TAF influence parameter χ indicated in the figure. The successful angiogenesis domain is always below the corresponding separation curve.

also be studied. At $t=0$, nutrient concentration is highest in the vicinity of the original vessels; as time evolves, a higher proportion of nutrients becomes available everywhere, with the maximum being shifted towards the tumor neighborhood.

Since experimental antiangiogenic therapies frequently focus on reducing the number of active TAF receptors, we examine the effects of varying the TAF absorption rate ζ, which is proportional to that number. This is done in Figs. 2–4. The snapshots in Fig. 2 depict the steady state for the same parameters as in Fig. 1, except that $\zeta=0.05$ in the first row, $\zeta=0.2$ in the second, and $\zeta=0.25$ in the third. The columns represent, respectively, the distributions of tubes, vessels, and free nutrients. The intermediate case, $\zeta=0.2$, is the most favorable for angiogenic development: in the second row, we see that c_2 has disappeared, whereas c_3 and p have their maxima near the tumor. If ζ is reduced, for instance, through the action of an antiangiogenic drug that binds to the TAF receptors, there is a weaker growth of new vessels and the increase in available nutrients occurs mostly in the neighborhood of the original vessels, being of no great relevance to the tumor (first row). Surprisingly, angiogenesis is also frustrated by the presence of too many TAF receptors: In the third row we see that a dense wall of tubes forms near the tumor edge, blocking the entrance of TAF to regions close to the original vessels and of nutrient to the tumor vicinity. Due to the lack of contiguity, they do not transform into c_3 cells. As a result, the angiogenic process fails, as evidenced by the low final concentration of free nutrients in the tumor neighborhood.

The linear plots in Fig. 3 confirm the view expressed in the preceding paragraph: Fig. 3(a) shows profiles of the distribution of available nutrients. These profiles were obtained by integrating p along the x direction, i.e., parallel to the tumor surface. We observe that, if $\zeta=0.2$, the nutrient distribution is biased towards the tumor, whereas it is more evenly (and thus less efficiently) distributed if $\zeta=0.025$ or $\zeta=0.04$, and it is constrained to the initial vessel neighborhood if either $\zeta=0.02$ (too few receptors) or 0.22 (too many). A different perspective is provided by Fig. 3(b): The total amount of nutrients reaching the tumor increases monotonically for intermediate values of ζ but, after an initial rise, it decreases abruptly when ζ is either too small or too large. Under these conditions, the proliferation of nutrient-consuming endothelial cells in the intervening region would starve the tumor completely. The sharp bend observed for intermediate values of ζ can be understood as follows: A temporary structure grows not too far from the tumor and shields the region between itself and the original vessels from TAF. Suddenly, the threshold is overcome at key locations and a very fast $c_2\rightarrow c_3$ transformation occurs.

The angiogenic efficiency e, defined in Eq. (16), is plotted in Fig. 4(a) as a function of ζ for several values of the threshold Q. In all cases, e is a monotonically increasing function of ζ. This was to be expected, because angiogenesis should be favored by an increase in the number of TAF receptors. The presence of the threshold increases the efficiency by limiting vessel consolidation (i.e., limiting c_3 proliferation) to regions where there is already a high density of ECs. As it was shown in Fig. 3(b), however, the simultaneous presence of a high concentration of TAF receptors and a threshold frustrates angiogenesis. Therefore, the lines terminate at lower values of ζ when Q is increased. On the other hand, a low concentration of TAF receptors makes it impossible to initiate angiogenesis if there is a finite threshold Q, because the required concentration of new ECs can never be reached. Figure 4(b) shows the region in the parameter plane (ζ,Q) where we predict successful angiogenesis for various values

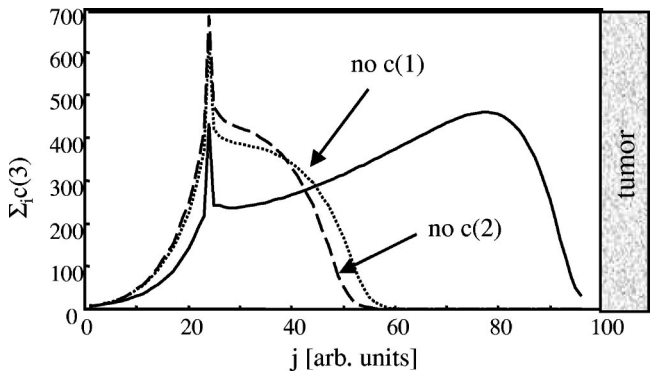

FIG. 5. Spatial distribution of vessel-forming ECs. Solid line, model considered in this paper; dashed line, simplified model with no tube formation; dotted line, simplified model with no diffusing cell formation. Only the complete model yields successful angiogenesis.

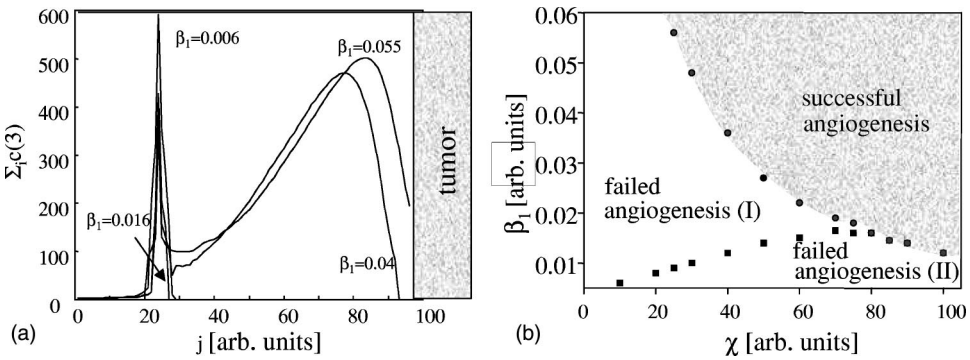

FIG. 6. Influence of TAF sensitivity. (a) Profiles of the c_3 distribution for the TAF influence parameter $\chi=40$ and the values of the signal dependent consumption rate β_1 specified next to the figures. (b) Successful and failed angiogenesis in the parameter plane (χ,β_1). See text.

of the TAF influence parameter χ. For each case the successful region is located under the curve. The size of this successful region grows monotonically with χ because cells that are highly sensitive to the TAF signal will redirect their energetic resources more efficiently towards angiogenic development.

We may ask if it is really necessary to consider three EC species. The answer is provided by Fig. 5, where we compare the c_3 profiles corresponding to the case of Fig. 1 with those corresponding to the same model when either the c_1 (dotted line) or the c_2 (dashed line) species is suppressed. The suppression of c_1 is in practice carried out by allowing newly formed c_1 cells to diffuse one step and then forcing them to transform immediately into c_2 cells. In both two-species cases we end up with a high concentration of new vessel growth around the initial vessel, which is nonconducive to successful angiogenesis. We conclude that, while the mobility of c_1 cells is required to ensure rapid growth away from the original vessels, the presence of the nonmigrating c_2 species is needed to reach concentrations high enough to permit the $c_2 \rightarrow c_3$ transformation.

The effect of EC sensitivity to TAF is explored in Fig. 6(a), where we present steady state c_3 profiles for $Q=0.3$, $\zeta=0.2$ and several values of β_1. For $\beta_1=0.04$ and $\beta_1=0.055$ we obtain successful angiogenesis. If β_1 is reduced to 0.016, there is no expansion of the vascular system. Data for intermediate times show that unstable structures form between the vessel and the tumor. The threshold Q impedes the consolidation of these structures, which block the diffusion of TAF towards the original vessel and frustrate vascular growth. However, if β_1 is further reduced, a different process takes place, with a strong growth of the vascular system in the immediate neighborhood of the original vessel. The effect of TAF is too weak to permit the growth of the blocking structures, but it suffices to generate, albeit very slowly, a marked amplification of the vascular system near the original vessel. This configuration is exhibited by the $\beta_1=0.006$ curve. There are therefore three regions in the parameter plane (χ,β_1), which are shown in Fig. 6(b). High values of both parameters favor successful angiogenic growth, but angiogenesis always fails for small values of χ. Very low values of β_1 give rise to the above-mentioned intense growth around the original vessels. Of course, strong, localized growth around the original vessels is unlikely: on one hand, growth would be limited by mechanical effects; on the other, if a vessel diameter grows substantially, its permeability will probably decrease, restraining growth.

The simple initial configuration (capillaries forming an inverted T near a flat tumor wall) was chosen in order not to obscure the parameter analysis with geometric factors. A more realistic example was presented in Ref. [14], where we set a circular tumor at the lattice center and observed the evolution of the microvessel density, which is proportional to c_3, from the original capillaries towards the tumor. The results were in qualitative agreement with observational data.

IV. CONCLUSIONS

We have developed a mathematical model that describes some of the fundamental processes involved in angiogenesis. The parameters we have defined can be used to quantify the importance of the various ingredients required by the angiogenic process. The model yields predictions that are in agreement with experimental observations. For instance, the predicted $\Sigma_i c_3(\vec{i})$ profiles for successful angiogenesis are in qualitative agreement with measured microvessel density values for lung carcinomas [12]. The model can be easily employed to predict the effect of a given therapy or combination of therapeutical courses specifically directed at the vascular system irrigating the tumor, once the suitable therapy-sensitive parameters are identified. In particular, we have already shown that it suggests an explanation for the observed synergy of some antiangiogenic therapies, indicating possible instances of synergic procedures [14].

Although we have not assumed that TAF has a direct chemotactic effect, we have seen that the extended vascular net grows towards the tumor. This directional growth is thus an emergent property of the model, which indicates that it is not necessary to assume that a given TAF has direct chemotactic properties to ensure the successful development of angiogenesis. Of course, direct chemotaxis can be incorporated in the model; if present, it will essentially speed up vascular growth. The influence of other processes on vascular growth can be also investigated in detail. It would be possible, for example, to analyze the effects of VEGF-increased vascular permeability [34], or to consider the upregulation by VEGF of its own receptors [35], the synergistic action of two or more angiogenesis promoters [4], or the stabilizing effect of VEGF [36]. We can also consider the simultaneous application of different therapeutical tools, investigating the possible emergence of synergistic action between molecular angiogenesis inhibitors and radiation [5] or surgical procedures.

In conclusion, we expect that this model will help to set the discussion of angiogenesis on a more quantitative footing. The increased precision furnished by the mathematical language should help in the interpretation of the action of antiangiogenic agents and in the optimization of antiangiogenic therapies.

ACKNOWLEDGMENTS

The authors are grateful to Professor P. P. Delsanto and Professor G. P. Pescarmona for useful discussions. This work was supported by CONICET and SECyT - UNC (Argentina), and by the INFM Parallel Computing Initiative (Italy).

[1] R.S. Kerbel, Nature (London) **390**, 335 (1997).
[2] T. Boehm, J. Folkman, T. Browder, and M.S. O'Reilly, Nature (London) **390**, 404 (1997).
[3] R.J.B. King, *Cancer Biology*, 2nd ed. (Pearson Education, Harlow, England, 2000).
[4] D. Hanahan and J. Folkman, Cell **86**, 353 (1996).
[5] H.J. Mauceri *et al.*, Nature (London) **394**, 287 (1998).
[6] W. Arap, R. Pasqualini, and E. Ruoslahti, Science **279**, 377 (1998).
[7] R. Cao *et al.*, Proc. Natl. Acad. Sci. U.S.A. **96**, 5728 (1999).
[8] P. Blezinger *et al.*, Nature (London) **17**, 343 (1999).
[9] M. Dhanabal *et al.*, J. Biol. Chem. **274**, 11 721 (1999).
[10] G. Bergers, K. Javaherian, K.-M. Lo, J. Folkman, and D. Hanahan, Science **284**, 808 (1999).
[11] J.M. Wood *et al.*, Cancer Res. **60**, 2178 (2000).
[12] M.I. Koukourakis *et al.*, Cancer Res. **60**, 3088 (2000).
[13] R.A. Brekken, J.P. Overholser, V.A. Stastny, J. Waltenberger, J.D. Minna, and P.E. Thorpe, Cancer Res. **60**, 5117 (2000).
[14] B. Capogrosso Sansone, M. Scalerandi, and C.A. Condat, Phys. Rev. Lett. **87**, 128102 (2001).
[15] J. Folkman and M. Klagsbrun, Science **235**, 442 (1987).
[16] W. Risau, Nature (London) **386**, 671 (1997).
[17] M.A.J. Chaplain, D.L. Benson, and P.K. Maini, Math. Biosci. **121**, 1 (1994).
[18] *A Survey of Models for Tumor-Immune System Dynamics*, edited by J.A. Adam and N. Bellomo (Birkhäuser, Boston, 1997).
[19] J. Smolle and H. Stettner, J. Theor. Biol. **160**, 63 (1993).
[20] S.C. Ferreira Junior, M.L. Martins, and M.J. Vilela, Physica A **261**, 569 (1998).
[21] M. Scalerandi, A. Romano, G.P. Pescarmona, P.P. Delsanto, and C.A. Condat, Phys. Rev. E **59**, 2206 (1999).
[22] A. Bertuzzi and A. Gandolfi, J. Theor. Biol. **204**, 587 (2000).
[23] P.P. Delsanto, A. Romano, M. Scalerandi, and G.P. Pescarmona, Phys. Rev. E **62**, 2547 (2000).
[24] C.A. Condat, B. Capogrosso Sansone, P.P. Delsanto, and M. Scalerandi, Recent Res. Dev. Biophys. Chem. (to be published).
[25] C.L. Stokes, D.A. Lauffenburger, and S.K. Williams, J. Cell. Sci. **99**, 419 (1991).
[26] M.J. Holmes and B.D. Sleeman, J. Theor. Biol. **202**, 95 (2000).
[27] A.R. Kansal, S. Torquato, G.R. Harsh IV, E.A. Chiocca, and T.S. Deisboeck, J. Theor. Biol. **203**, 367 (2000).
[28] See, for example, A. Sánchez, E.M. Nicola, and H. Wio, Phys. Rev. Lett. **78**, 2244 (1997); C.A. Condat and G.J. Sibona, Recent Res. Dev. Stat. Phys. **1**, 61 (2000); H. Taitelbaum and Z. Koza, Physica A **285**, 166 (2000), and references therein.
[29] P.P. Delsanto *et al.*, Wave Motion **16**, 65 (1992).
[30] G. Kaniadakis, P.P. Delsanto, and C.A. Condat, Math. Comput. Modell. **17**, 31 (1993).
[31] F. Schweitzer, W. Ebeling, and B. Tilch, Phys. Rev. Lett. **80**, 5044 (1998).
[32] I. Derényi, M. Bier, and R. Dean Astumian, Phys. Rev. Lett. **83**, 903 (1999).
[33] C.A. Condat and G.J. Sibona (unpublished).
[34] D.R. Senger, Am. J. Pathol. **149**, 1 (1996).
[35] J.M. Isner and T. Asahara, J. Clin. Invest. **103**, 1231 (1999).
[36] N. Ilan, S. Mahooti, and J.A. Madri, J. Cell. Sci. **111**, 3621 (1998).